Coastal Dynamics 2017
Paper No. 104

FORMATION OF SHARP BREAK IN SLOPE BETWEEN FORESHORE AND LOW-TIDE TERRACE AND LONGSHORE CHANGE IN HEIGHT OF SHARP BREAK

Yasuhito Noshi[1], Akio Kobayashi[1], Takaaki Uda[2] and Yoshiki Hashimoto[1]

Abstract

A foreshore and tidal flat are separated by a sharp break in the slope. A field investigation was carried out on the Nako-Funakata coast in Tateyama Bay to study its characteristics. It was found that the berm crest line obliquely intersected with the low-tide shoreline. The formative mechanism of such a topography was investigated using the BG model considering the effect of the change in grain size. The formation of the oblique intersection of the berm crest line to the low-tide shoreline was explained by the difference in sand movement around a groin: coarse material was effectively blocked by the groin, whereas fine material was transported offshore of the groin by longshore sand transport, which was induced by the wave-sheltering effect of an offshore breakwater.

Key words: break in slope, foreshore, tidal flat, Nako-Funakata coast, field observation, BG model, groin effect

1. Introduction

A tidal flat is formed by the successive deposition of fine materials supplied from rivers in a tidal area, and a vast flat area with a gentle slope of approximately 1/1,000 is formed offshore of the coastline. These tidal flats are an important habitat for various sea animals and seashells, and therefore much attention has been paid to their preservation. Similarly to the development of tidal flats in a tidal area, even in a wave-dominated area, a tidal flat composed of fine sand can be formed. The beach changes in such a tidal flat differ from those of a coast exposed to rough waves in open oceans, although there have been a few studies on such beach changes. Uda et al. (2008) investigated the formative mechanism and deformation of a sand bar in the Sanbyakken area facing Nakatsu tidal flat in Oita Prefecture by field investigation and found that a foreshore composed of coarse sand and a tidal flat composed of fine sand intersect with a sharp break in the slope. Similar characteristics were also measured in a field investigation on the marginal coast of Banzu tidal flat in Tokyo Bay (Tohbara et al., 2015) and on the marginal coast on the Nakatsu tidal flat facing the Suo-nada Sea (San-nami et al., 2015). Although a sharp break in the slope is formed along the boundary between the foreshore and the tidal flat, its height may change alongshore and may be related to the wave conditions or the grain size of the bed material. However, this has been hardly studied. Here, we carried out a field investigation on the Nako-Funakata coast facing Tateyama Bay, where both a sandy beach and a tidal flat coexist. On the basis of this field observation, the beach changes were reproduced using the BG model, which considers the effect of the change in grain size (Noshi et al., 2010).

2. METHOD OF FIELD INVESTIGATION

The Nako-Funakata coast is a sandy beach with a length of 1.5 km extending north of the Heguri River mouth, as shown in Fig. 1. Funakata fishing port is located at the north end of the coast, and an offshore breakwater of 300 m length was constructed offshore of the fishing port breakwater. In this study, the reference point was fixed at the south end of the seawall on the right bank of the Heguri River mouth, and

[1]Nihon University, 7-24-1 Narashinodai, Funabashi, Chiba 274-8501, Japan. kobayashi.akio@nihon-u.ac.jp, noshi.yasuhito@nihon-u.ac.jp
[2]Head, Shore Protection Research, Public Works Research Center, 1-6-4 Taito, Taito, Tokyo 110-0016, Japan. uda@pwrc.or.jp

the X-axis was taken alongshore from this reference point and the Y-axis normal to the X-axis. On the Nako-Funakata coast, sand supplied from the Heguri River has been transported by northward longshore sand transport and deposited around the fishing port (Sugawara et al., 2009). To reduce the volume of sand deposited immediately south of the fishing port, an impermeable, stone-made groin with 65 m length was constructed at $X = 1$ km, which was completed in November 2014.

Field observation was carried out on May 2, July 30, and October 13, 2015. In the field observation, the low-tide shoreline, the intersection line between the foreshore and the low-tide terrace, and the berm crest line were measured by the GPS (Garmin Co. Ltd.: GPS map 62scj). The intersection line between the foreshore and the low-tide terrace corresponds to the boundary line where the beach slope abruptly changes from a steep slope of 1/10 with the foreshore composed of coarse sand or medium-size sand to the low-tide terrace with a gentle slope of approximately 1/100, as schematically shown in Fig. 2. The elevation of the point of the sharp break in the slope was measured on October 13, 2015. The foreshore slope and the slope of the low-tide terrace were measured on May 2, 2015.

Figure 3 shows the locations of the sampling points of the foreshore and low-tide terrace. The foreshore material was sampled at Sts. 1-20 and at Sts. 6'-20' on the low-tide terrace. The sampled material was dried and sieve analysis was carried out to investigate the grain size composition. The elevation of the point of the break in the slope was measured along the intersection line between the foreshore and the low-tide terrace using an RTK-GPS (Trimble R4).

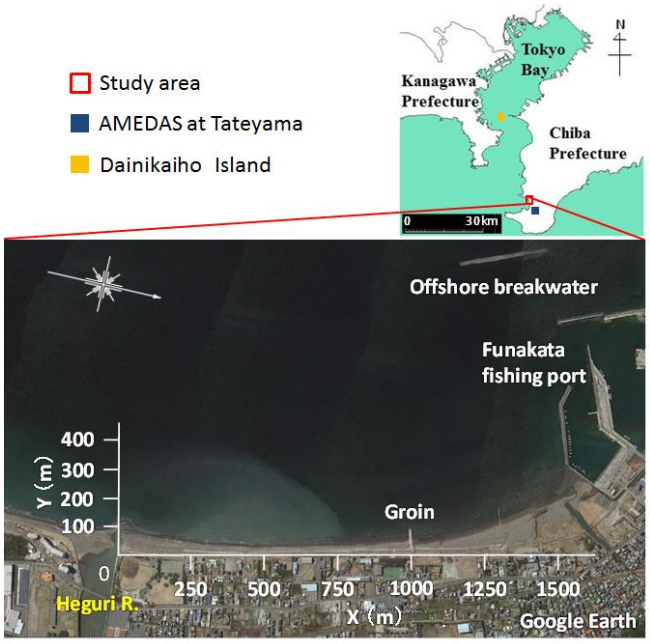

Figure 1. Location of Nako-Funakata coast and coordinate system.

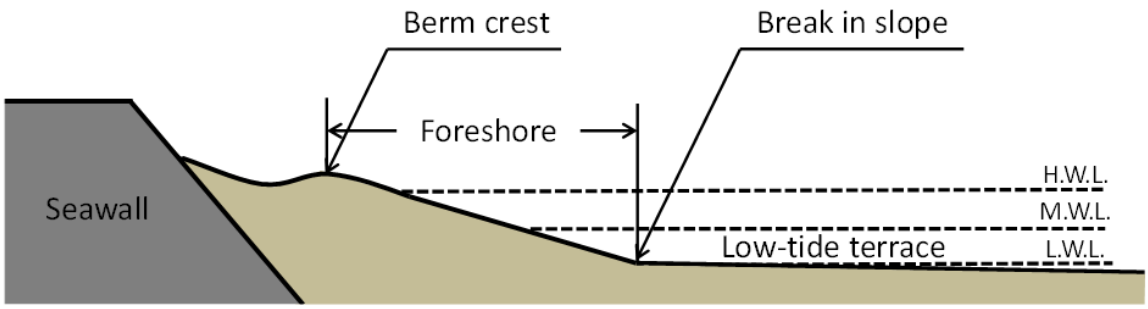

Figure 2. Definitions of height of berm crest, sharp break in slope, and low-tide terrace.

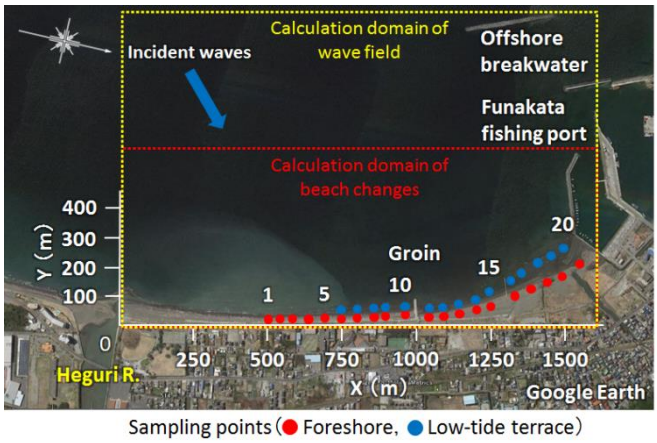

Figure 3. Sampling points on foreshore and low-tide terrace.

3. TIDE AND WAVE CONDITIONS AT NAKO-FUNAKATA COAST

Because the Nako-Funakata coast is located in Tateyama Bay, the tide data at Tateyama Port can be used for reference: the high- and low-tide levels are +0.73 m and -0.85 m above mean sea level (MSL), respectively. Since the coast approximately faces W, as shown in Fig. 1, wind waves from the west are predominant. Referring to AMEDAS data taken between 2010 and 2014 at Tateyama Meteorological Station, the probability of occurrence of the wind direction at the Nako-Funakata coast is shown in Fig. 4. Because the shoreline of this coast almost runs in the south-north direction, the predominant wind direction is SW throughout the year with a slight variation between SSW and WSW.

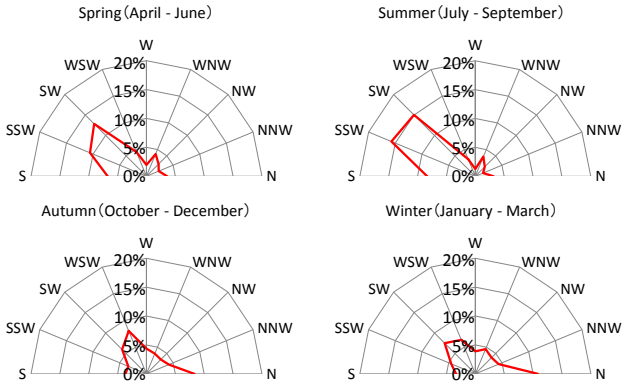

Figure 4. Wind rose for Tateyama from AMEDAS data measured between 2010 and 2014.

4. RESULTS OF FIELD INVESTIGATION

4.1. *Field observation*

Topographic features around a groin on the coast were investigated on April 18, 2015. First, Fig. 5 shows the sandy beach and low-tide terrace in the area north of the groin. The foreshore slope is approximately 1/10, and the flat low-tide terrace is clearly separated by a sharp break in the slope. Figure 6 is the south view from the top of the groin. The low-tide terrace with a gentle slope extends between the foreshore and the low-tide shoreline, and its width gradually decreases to the south. Figure 7 shows the berm crest line taken from the top of the groin and the wide foreshore immediately south of the groin.

Figure 5. Foreshore, sharp break in slope, and low-tide terrace north of groin.

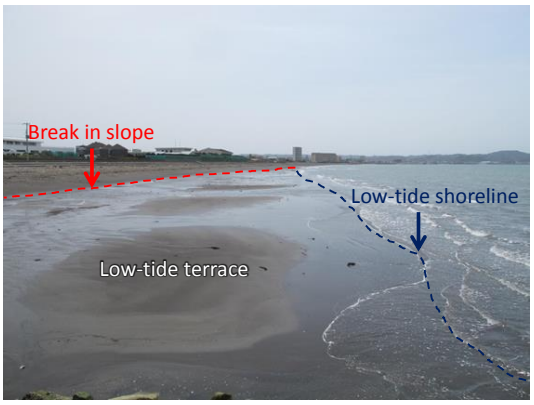

Figure 6. Low-tide shoreline and terrace south of groin.

Figure 7. Berm crest line south of groin.

4.2. *Low-tide shorelines, intersection line between foreshore and low-tide terrace, and berm crest line*

Figure 8 shows the longshore configuration of the low-tide shoreline, the intersection line between the foreshore and the low-tide terrace with the sharp break in the slope, and the berm crest line measured on May 2, July 30, and October 13, 2015, respectively. The intersection line runs approximately parallel to the berm crest line, and the interval between the intersection line and the low-tide shoreline, i.e., the width of the low-tide terrace, gradually increases northward from the Heguri River mouth. Furthermore, because the low-tide shoreline at the tide level of -0.42 m has a gap on both sides of the groin with shoreline recession on the north side, longshore sand transport along this contour is considered to be partially blocked by the

groin. On the other hand, the low-tide shorelines at tide levels of -0.77 and -0.83 m extend continuously across the tip of the groin while allowing continuous sand movement around the tip of the groin, implying that the point depth of the groin is approximately -0.8 m above MSL.

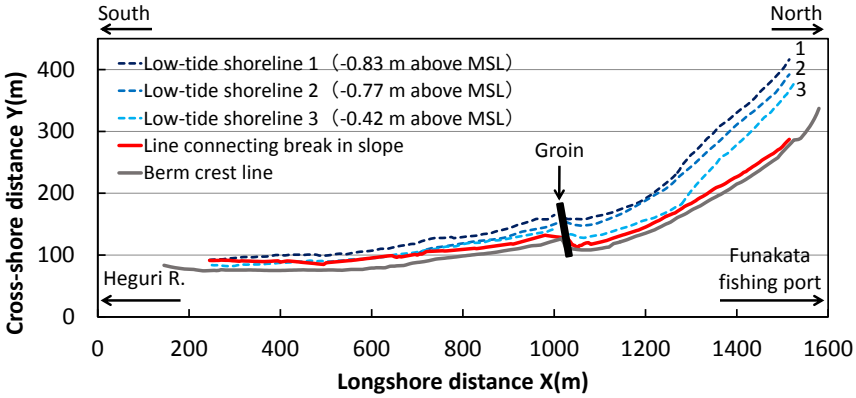

Figure 8. Longshore distribution of berm crest line, line connecting break in slope, and low-tide shoreline.

4.3. *Elevations of point of break in slope and berm crest*

The measured elevations of the point of the sharp break in the slope and the berm crest are shown in Fig. 9. Here, the elevation of the berm crest was calculated from the elevation of the point of the break in the slope, the foreshore slope, and the foreshore width. Although the berm height increases from $X = 830$ m to the groin, except in the immediate vicinity of the groin because of the large variations near the groin, it varies around 1.1 m north of the groin and tends to decrease northward from the Heguri River mouth to the fishing port. This is considered to correspond to the northward reduction in the wave height due to the wave-sheltering effect of the offshore breakwater of Funakata fishing port. Although the height of the point of the break in the slope generally increases northward, it takes small values locally at locations a, b, and c at the mouths of the drainage channels north of the groin. In particular, the height is very low in front of drainage channel b. This reduction of the elevation of the point of the break in the slope is assumed to be due to the effect of seaward currents from the drainage channel.

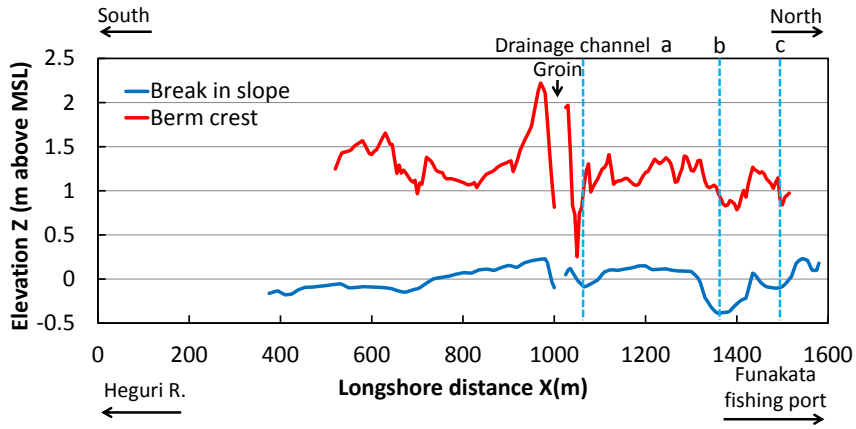

Figure 9. Elevations of point of break in slope and berm crest.

4.4. *Widths of foreshore and low-tide terrace*

Figure 10 shows the foreshore width and that of the low-tide terrace measured on July 30, 2015, which

were defined as the cross-shore distance between the berm crest and the point of the break in the slope, and the distance between the break in the slope and the low-tide shoreline, respectively. The foreshore width gradually decreases from 16 m at the Heguri River mouth to 9 m at the north end. In contrast, the width of low-tide terrace markedly increases north of the Heguri River mouth and reaches a maximum of 130 m at X = 1,515 m near the fishing port.

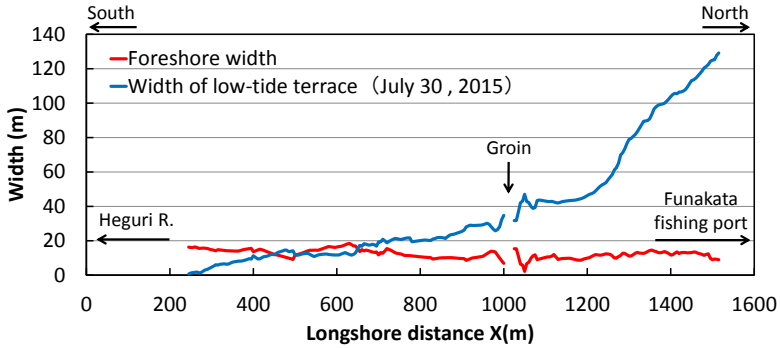

Figure 10. Foreshore width and width of low-tide terrace.

4.5. *Foreshore slope, slope of low-tide terrace, and grain size distribution*

Figure 11 shows the longshore changes in the slopes of the foreshore and low-tide terrace. Although the foreshore slope rapidly increases from St. 7 to St. 10 immediately south of the groin, it has an almost constant value of 1/10 outside this area. The slope of the low-tide terrace is approximately 1/50 south of the groin, whereas north of the groin it decreases to as low as 1/100, implying that a very gentle seabed extends as a tidal flat in the offshore zone. Figure 12 shows the longshore distributions of the content of each grain size of the materials on the foreshore and low-tide terrace. On the foreshore, there is no significant difference in the content on both sides of the groin, and medium-size sand is the major component at approximately 50% with the remainder comprising fine and coarse sand. In contrast, on the low-tide terrace, although the content of medium-size sand exceeds 80% at St. 6' south of the groin, it decreases to 45% near the groin as Sts. 7', 8' and 9' with a gradual increase in the content of fine sand to 55%.

On the low-tide terrace north of the groin, the content of fine sand is as high as 60%, with the exception of St. 17' where the content of medium-size sand locally increases to 90% because of the inflow of a small river. As general characteristics, the content of coarse sand is approximately 75% with the content of fine sand less than 25% on the foreshore, whereas the content of fine sand reaches as high as 75% with a content of 25% of coarse sand on the low-tide terrace.

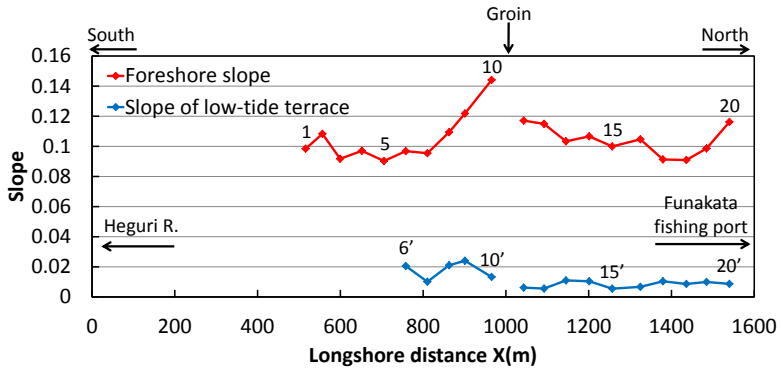

Figure 11. Longshore distributions of foreshore slope and slope of low-tide terrace.

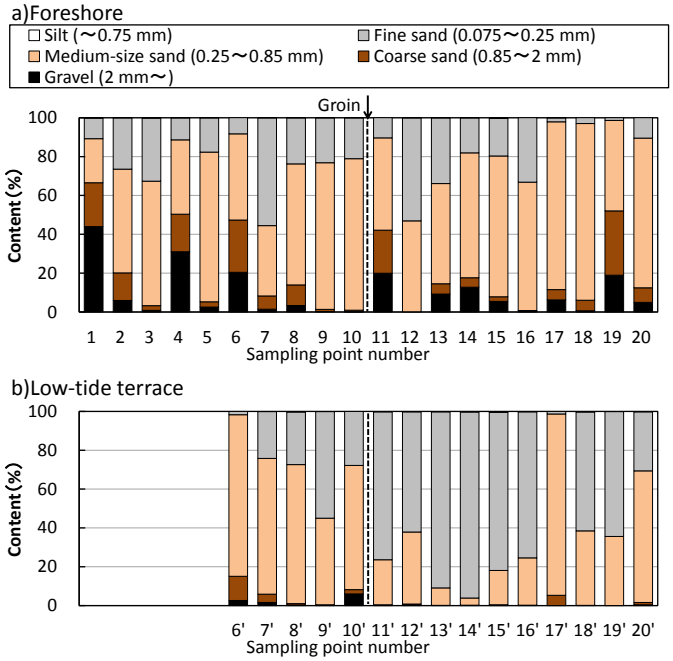

Figure 12. Grain size distributions of beach materials on foreshore and low-tide terrace.

5. NUMERICAL SIMULATION OF INTERSECTION OF BERM CREST LINE WITH LOW-TIDE SHORELINE

The reason for the oblique intersection of the berm crest line with the low-tide shoreline is considered using the schematic diagram shown in Fig. 13. On this coast, a wave-shelter zone is formed by the offshore breakwater, and longshore sand transport from the vicinity of the Heguri River outside the wave-shelter zone to inside the zone is induced by the wave-sheltering effect of the offshore breakwater. In this case, relatively coarse sand is transported northward along the foreshore because of the large equilibrium slope, and such longshore sand movement is effectively blocked by the groin. In contrast, fine sand is transported northward in a wider offshore area while being deposited with a gentle slope. Thus, the littoral zone for fine sand is so wide that the blocking effect of the short groin is small, allowing the movement of fine sand around the tip of the groin. As a result of the selective movement of the fine sand, the coarser material is left upcoast, whereas the fine sand is selectively deposited in the northern part. The appropriateness of this assumed mechanism was validated using the BG model.

Because the foreshore and low-tide terrace are mainly composed of grains of two different size components, as shown in Fig. 12, the calculation was carried out assuming that the beach materials are composed of grains with two sizes: medium-size sand of d = 0.3 mm with an equilibrium slope of 1/10 and fine sand of d = 0.1 mm with an equilibrium slope of 1/100 with contents of 25% and 75%, respectively. Sand with a mixed grain size is assumed to be transported while being subjected to the sorting effect of the grain size, resulting in the grain size distribution shown in Fig. 12. When waves are incident to the beach with a uniform slope composed of sand with the mixed grain size, the medium-size sand and fine sand are transported shoreward and seaward, respectively, because the equilibrium slope significantly differs for two grain sizes, resulting in the formation of a longitudinal profile in which the foreshore and low-tide terrace are separated by the point of the sharp break in the slope.

As the initial topography used in the numerical simulation, a model beach with a uniform slope of 1/50 extending between a berm height of 1.5 m and an offshore low-tide terrace of 2 m depth was assumed, as shown in Fig. 14, and the stable beach topography was calculated under the condition that waves with a significant wave height of 0.5 m (wave period 3.5 s) were incident to this initial topography for 10 days, a

sufficiently long period to observe beach changes. The wave height and wave period used in the calculation were determined as the annual mean of the NOWPHAS observation results in 2014 offshore of Daini-kaiho Island in Tokyo Bay, located at point P 30 km north of the study site, although these values may have been underestimating, because the wave observation site is located in Tokyo Bay. In Fig. 14, although the offshore seabed is assumed to be flat with a constant depth of 2 m, beach changes can take place when sand is transported and deposited on this flat sea bottom. Table 1 shows the calculation conditions. Here, although there is a tide change of 0.85 m on the study coast and the point depth of the groin changes with time, the effect of the tide change was neglected to enable the long-term prediction of beach changes.

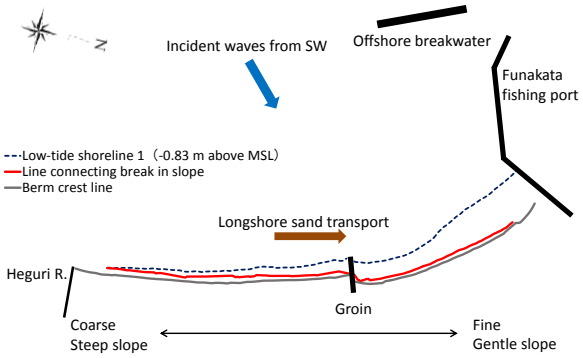

Figure 13. Schematic explanation of beach changes on Nako-Funakata coast.

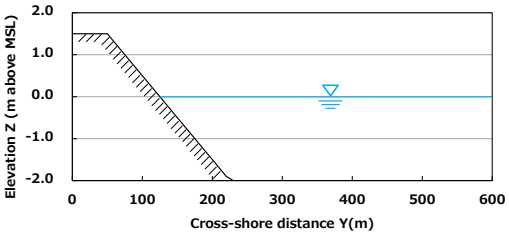

Figure 14. Initial longitudinal profile with uniform slope.

Table 1. Calculation conditions.

Numerical model	**BG model considering change in grain size proposed by Noshi et al. (2010)**
Initial topography	Stable beach formed when waves are incident to the beach with parallel contours
Equilibrium slope	1/10 (medium-size sand, d = 0.3 mm), 1/100 (fine sand: d = 0.1 mm)
Sea level	M.S.L. 0.0 m
Wave conditions	Significant wave height H: 0.5 m, wave period T: 3.5 s, wave direction: SW
Depth range of beach changes	Berm height h_R = 1.5 m Depth of closure h_C = 3 m
Coefficient of sand transport	Coefficient of sand transport A = 0.3, Coefficient of Ozasa and Brampton's term ζ = 1.62, coefficient ratio of cross-shore to longshore sand transport K_Z/K_X = 0.1
Depth distribution of sand transport	Uniform
Critical slopes of falling sand	1/2 on land, 1/3 on seabed
Calculation domain	X = 0 -1.6 km in longshore direction, Y = 0 - 0.6 km in cross-shore direction
Mesh sizes	ΔX = 20 m, ΔY = 10 m
Time interval	Δt = 1 hr
Total time steps	1 yr: 8,760 steps

Figure 15(a) shows the results of the calculation. This beach has a uniform profile in the longshore direction. Medium-size sand concentrated on the foreshore, forming a steep slope, whereas fine sand was deposited in the offshore zone, forming a gentle slope of 1/100. Figure 15(b) shows the corresponding grain size distribution on the beach, where fine sand of grain size 0.1 mm is deposited in the offshore zone, whereas medium-size sand of grain size 0.3 mm is accumulated on the foreshore.

The wave field was calculated given a significant wave height of 0.5 m incident from SW using the angular spreading method for irregular waves (Sakai et al., 2006), assuming that an offshore breakwater is installed in the offshore area of the beach, as shown in Fig. 15, with a uniform profile alongshore. Figure 16 shows the calculated planar distributions of the wave height and wave direction. The wave height gradually decreases northward because of the wave-sheltering effect of the offshore breakwater, and waves are incident obliquely to the shoreline with a larger wave angle in the north part.

The beach topography and grain size distribution after one year of wave action on the initial topography in Fig. 15 are shown in Fig. 17 for the wave field in Fig. 16. Although the low-tide shoreline obliquely extends northward in the area south of the groin, the berm crest line extends parallel to the X-axis near the groin in the calculated bathymetry, resulting in the oblique intersection between the berm crest line and the offshore low-tide shoreline. In the north part of the groin, the low-tide shoreline markedly advances northward from the groin, whereas the advance in the berm crest line is small, and both intersect similarly to in the south area. These results convincingly explain the measured results shown in Fig. 8.

Owing to the grain size distribution, as shown in Fig. 17(b), the medium-size sand formed a narrow band along the foreshore, whereas fine sand was deposited on the low-tide terrace. This again explains the measured grain size distribution. Figure 18 shows longitudinal profiles at 200 m intervals between $X = 0.4$ and 1.6 km. The elevation of the break in the slope between the foreshore and the low-tide terrace gradually increases between $X = 0.4$ and 1.54 km, and between $X = 1.4$ and 1.6 km, the elevation has a constant value. This distribution is in good agreement with the measured results shown in Fig. 9.

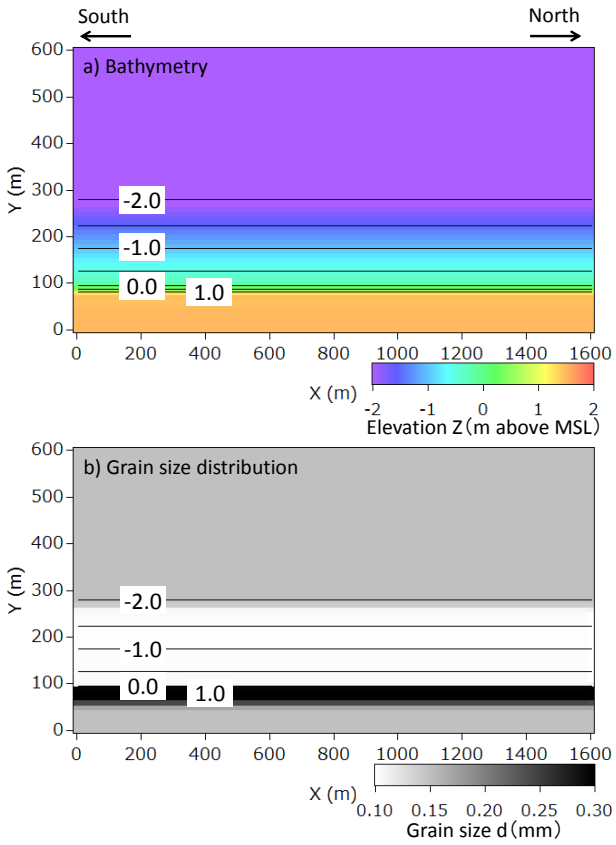

Figure 15. Initial bathymetry and grain size distribution.

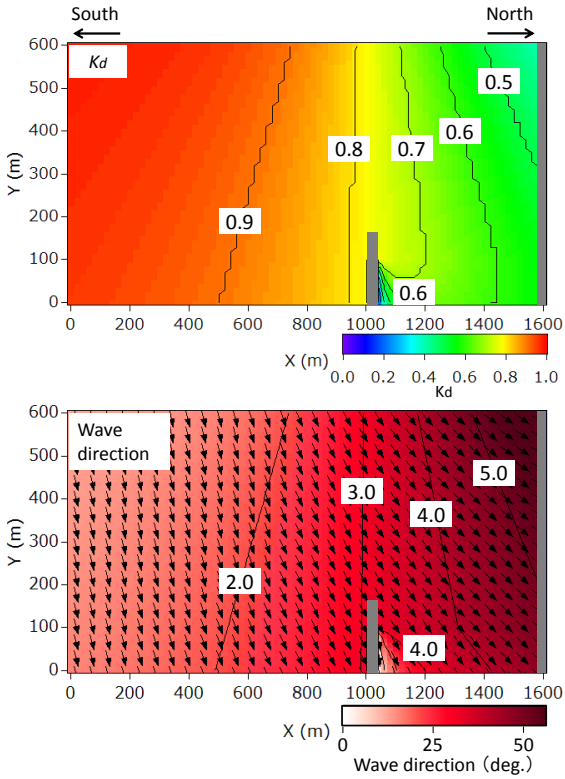

Figure 16. Distributions of wave height and wave direction calculated using angular spreading method for irregular waves.

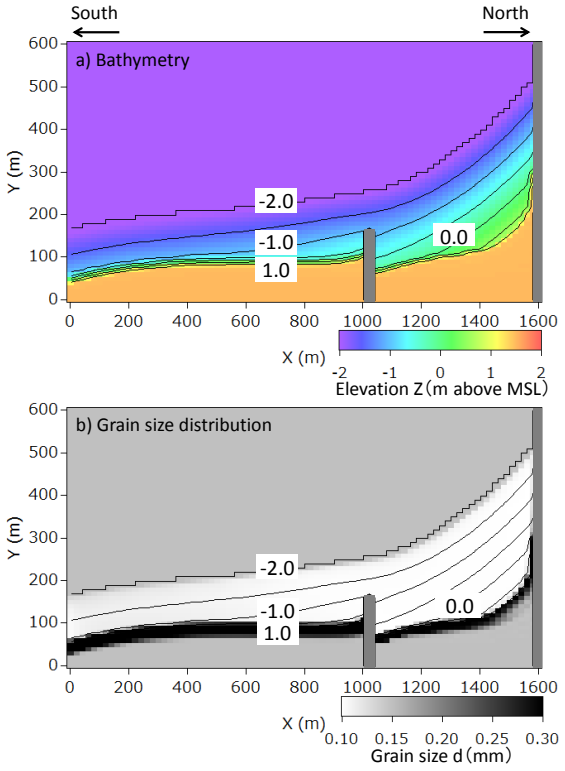

Figure 17. Predicted bathymetry and grain size distribution after one year of wave action.

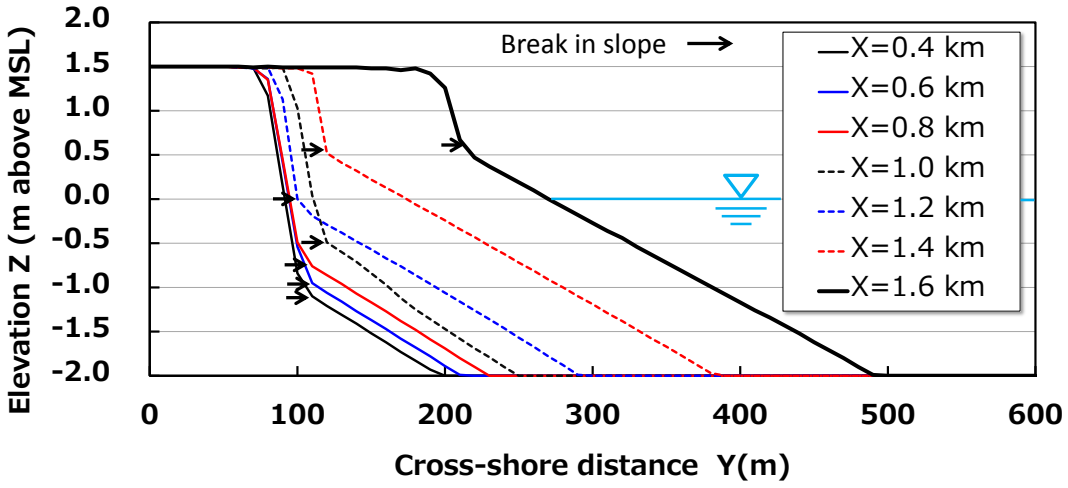

Figure 18. Superimposed profiles.

6. CONCLUSIONS

The oblique intersection of the boundary line between a foreshore and a low-tide terrace with the low-tide shoreline was investigated by field observation, taking the Nako-Funakata coast in Tateyama Bay, Japan, as an example. Then, three-dimensional beach changes and grain size changes of the seabed material of this coast were predicted, taking into account the wave-sheltering effect due to the offshore breakwater of Nako-Funakata fishing port, using the BG model, which considers the effect of the change in grain size on the longitudinal profile proposed by Noshi et al. (2010). It was found that the oblique intersection of the boundary line between the foreshore and low-tide terrace with the low-tide shoreline resulted under such conditions: longshore sand transport took place owing to the wave-sheltering effect of the offshore breakwater of the fishing port, and the groin blocked the movement of coarse sand, which concentrates along the shoreline, whereas fine sand was transported offshore of the groin, allowing its movement around the tip of the groin.

References

Noshi, Y. Uda, T. Serizawa, M. Kumada, T. and Kobayashi, A., 2010. Model for predicting bathymetric and grain size changes based on Bagnold's concept and equilibrium slope corresponding to grain size composition, Proc. 32nd *ICCE*, sediment.15, pp. 1-13.
http://journals.tdl.org/ICCE/article/view/1075/pdf_177

Sakai, K. Uda, T. Serizawa, M. Kumada, T. and Kanda, Y., 2006. Model for predicting three-dimensional sea bottom topography of statically stable beach, Proc. 30th *ICCE*, pp. 3184-3196.

San-nami, T. Uda, T. Miyahara, S. and Serizawa, M., 2015. Deformation of an isolated offshore sand bar on tidal flat and mergence with beach due to waves, *Coastal Sediments* '15, CD-ROM, No. 14, pp. 1-14.

Sugawara, Y. Kobayashi, A. Uda, T. Sakai, K. and Kurosawa, Y., 2009. Beach erosion triggered by anthropogenic factors - example of Funakata coast in Chiba Prefecture, Proc. *Civil Eng*. in the Ocean, JSCE, Vol. 25, pp. 1185-1190. (in Japanese)

Tohbara, H. Kobayashi, A. Uda, T. Mikami, Y. and Noshi, Y., 2015. Field investigation of beach changes along marginal shoreline of Banzu tidal flat, J. JSCE (B3 *Civil Eng*. in the Ocean), Vol. 71, No.2, pp. I_293-I_298. (in Japanese)

Uda, T. Seino, S. Ashikaga, Y. and Jono, H., 2008. Annu. J. of Japan. *Coastal Eng*., Vol. 55, pp. 481-485. (in Japanese)